Nanoscale

Accepted Manuscript

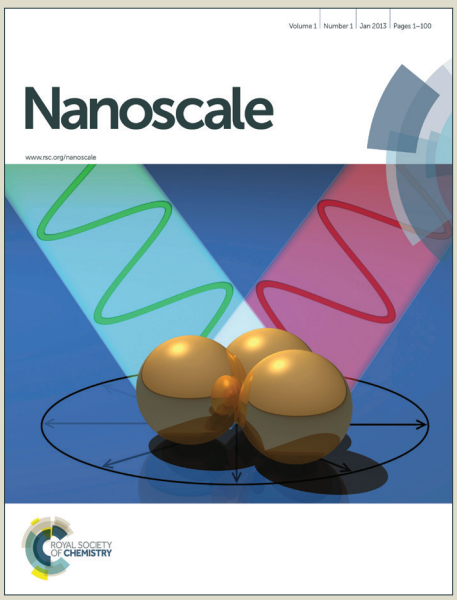

ROYAL SOCIETY OF CHEMISTRY

www.rsc.org/nanoscale

A generic amplification strategy for electrochemical aptasensors using a non-enzymatic nanoceria tag

*Gonca Bulbul, Akhtar Hayat, and Silvana Andreescu**

Department of Chemistry and Biomolecular Science,
Clarkson University, Potsdam, NY, USA.
Fax: 3152686610; Tel: 3152682394.

*Corresponding author E-mail: eandrees@clarkson.edu

Abstract

We report a novel non-enzymatic nanocatalyst based approach to construct an electrochemical aptasensor involving the synergistic contribution of a nanoceria (nCe) tag and graphene oxide (GO). The aptamer was immobilized on the surface of a GO modified electrode. The target analyte was captured by the immobilized aptamer via a specific competitive mechanism between the free and nCe labeled target. The electrochemical signal was generated by monitoring the electro-oxidation of a generic redox species upon reaction with the nCe tag. The signal was further amplified by the GO layer used as an electrode material to immobilize the aptamer and to increase the electron transfer at the electrode surface, further enhancing sensitivity of the assay. This strategy provides a universal platform for sensitive and specific detection of a wide spectrum of aptamer targets. Application of this new design for the electrochemical detection of Ochratoxin A (OTA) is demonstrated. Under optimal conditions, the aptasensor exhibited a linear response to OTA in the range 0.15 -180 nM with a detection limit of 0.1 nM. The method has been successfully used for the detection of OTA in cereal samples. This design may offer a new methodology for sensitive and specific detection of a wide spectrum of analytes for medical, environmental and electronic applications.

Keywords: nanoceria tag, aptamer, graphene oxide, electrochemical techniques, biomimetic label

Graphical abstract

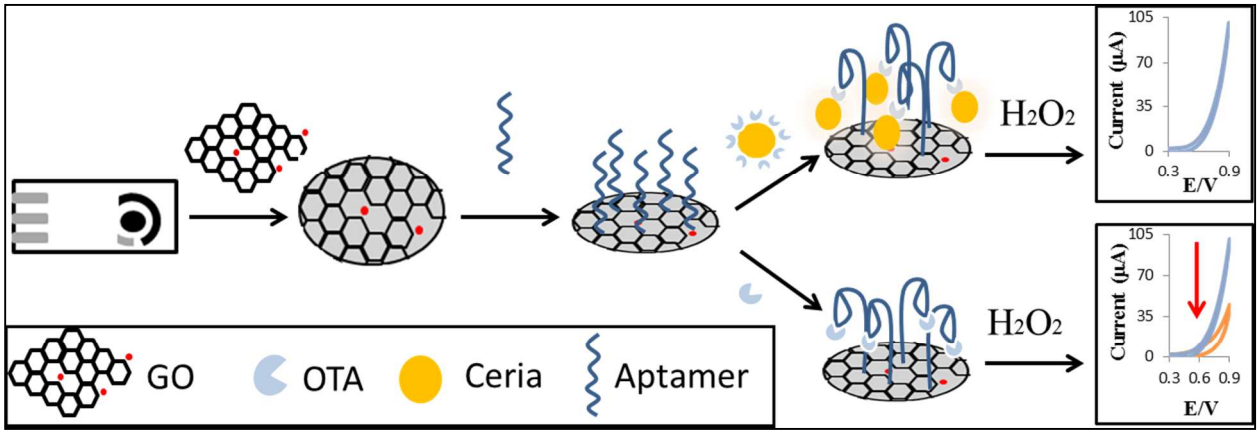

Highlight: A generic strategy for the fabrication of electrochemical aptasensors involving a non-enzymatic nanoceria tag and graphene oxide for sensitive and inexpensive detection of aptamer targets.

1. Introduction

The development of aptamer based biomolecular recognition assays has received significant interest over the past decade. Aptamers are functional short single stranded nucleic acid ligands which have a high specific binding ability to their target. Their advantages include chemical stability, cost effectiveness and ease of modification for detection and immobilization in sensing design.[1-3] Aptamers are synthesized in vitro, eliminating the need of animal or cell cultures and enabling production of non-immunogenic and toxic targets that cannot be acquired by the immune system.[4] These unique features make them interesting molecular recognition probes and possible replacements for conventionally used antibodies. Most traditional aptasensors employ an enzyme label to achieve the required detection sensitivity. However, the use of enzymes increases cost and limits the stability of the assay. The most sensitive assays are those with electrochemical detection that often incorporate redox mediators, further increasing complexity. Herein, we propose a novel electrochemical aptasensor design that utilizes redox active cerium oxide nanoparticles, or nanoceria (nCe), as a label for detection of molecular binding events in a competitive assay format. We use graphene oxide (GO) as an electrode material to facilitate the electron transport[5-6] and to enhance the electrochemical response due to its high conductivity[7] and peroxidase-like activity.[8] The synergistic enzyme-like activity of nCe and GO provides catalytic enhancement thus increasing the detection sensitivity of the assay. Furthermore, by replacing both the enzyme label and the electron mediator with more stable inorganic alternatives, target analytes can be detected with high sensitivity using a robust, less complex and inexpensive procedure.

nCe particles have received significant scientific interest because of their catalytic and free radical scavenging properties. nCe has been shown to exhibit catalase and oxidase-like activity in aqueous environments due to the presence of cerium in dual oxidation states ($Ce^{3+/}Ce^{4+}$) which enables these particles to act both as an oxidation and reduction catalyst.[9-11] We have used this property to fabricate ceria-based electrochemical sensors for the detection of H_2O_2,[12] in enzyme sensors that are able to operate in oxygen restrictive environments[13] and as signal amplifiers in alkaline phosphatase assays.[14] Here, we extend the application of nCe particles to create a universal electrochemical aptasensor that can be used as a general platform for the detection of molecular binding events with high sensitivity and stability. Moreover, recent

reports have demonstrated the peroxidase-like activity of carboxyl graphene oxide that, when used synergistically with the biomimetic nature of nCe can significantly increase assay sensitivity. To the best of our knowledge, this is the first time redox active nanoparticles have been integrated and used as a label in electrochemical aptasensors. The electrochemical signal is generated by monitoring the electro-oxidation of hydrogen peroxide (H_2O_2) upon redox reaction with nCe. The signal is further amplified by the carboxyl GO layer used as an electrode material to immobilize the aptamer, and also to increase the electron transfer rate at the electrode surface.

To demonstrate this principle, we have designed a nCe based aptasensor to detect Ochratoxin A (OTA) a low molecular weight mycotoxin, selected here as a model example. OTA is produced by filamentous fungi of *Aspergillus* and *Penicillium,* which is characterized by high toxicity at very low concentrations. OTA is known to contaminate a wide variety of food matrices such as cereals, dried fruits, coffee, cocoa, spices, beer, wine and grape juice.[15] OTA has been suggested to contribute to the development of cancer by the International Agency for Research on Cancer (Group 2B) and has been considered nephrotoxic, teratogenic and immunosuppressive.[16] Due to the presence of OTA in food products and its high toxicity at low concentrations, there is a demand for highly sensitive and selective detection methods to determine exposure levels and minimize the potential risk to human health and the environment. Although a specific application is demonstrated, this sensor design can also be applied for the detection of other targets in the environmental, food and clinical monitoring fields.

2. Experimental

2.1. Materials and reagents

Cerium oxide (IV) or nCe particles, 20 wt% colloidal dispersion in 2.5% acetic acid with an average size of 20–25 nm were purchased from Sigma Aldrich. The OTA specific, 5'-amino-modified aptamer strand was synthesized by Eurogentec (North America Inc). The sequence for the given strand is provided in the Table 1. Graphene was obtained from Angstron Materials. OTA was obtained from Santa Cruz Biotechnology. Ochratoxin B (OTB) was from Cayman Chemical Company. OTA and OTB were first dissolved in ethanol and then diluted in binding buffer. All solutions were prepared with deionized Milli-Q water (Millipore, Bedford, MA,

USA.). A buffer solution at pH 7.4 containing 1mM $MgCl_2$, 140 mM NaCl, 2.7 mM KCl, 0.1 mM Na_2HPO_4 and 1.8 mM KH_2PO_4 was used as a binding medium. The components (ACS grade) of the binding buffer including $MgCl_2$, NaCl and KCL were purchased from Fisher Scientific, Na_2HPO_4 was from Acros, KH_2PO_4 was from Sigma Aldrich. Sulfuric acid and nitric acid from Fisher Scientific were used for carboxylation of graphene. Potassium ferricyanide was from J.T. Baker. 1-(3-Dimethylaminopropyl)-3-ethylcarbodiimide hydrochloride (EDC) was obtained from Tokyo Chemical Industry CO., LTD. Faradaic impedimetric measurements were carried out in 0.1 M phosphate buffer saline (PBS) at pH 7.4 containing 1 mM potassium ferricyanide ($K_3[Fe(CN)_6]$) within the frequency range of 1 Hz-100 kHz, an ac amplitude of 0.1 V, and a bias dc during the run below 1 Hz.

2.2. Apparatus

UV–vis spectrophotometric measurements were performed with a Schimadzu P2041 spectrophotometer equipped with a 1-cm path length cell. Electrochemical experiments were carried out with a CHI model 660 potentiostat (CH Instruments, Austin, TX) connected to a conventional three electrochemical cell. Impedimetric studies were done with a CHI model 920C potentiostat (CH Instruments, Austin, TX). Screen printed carbon electrodes (SPCE) (DRP 110) from DropSens (Spain) were used for cyclic voltammetry and impedance studies.

2.3. Modification of GO

Functionalized GO was prepared using the carboxylation process described by Chhabra et al, which has been shown to yield high carboxylated graphene.[17] 5 mg of graphene was used, 3.5 mg of which was added to 15 ml H_2SO_4 and the remaining 1.5 mg was added to 5 ml HNO_3 (3:1 ratio 15 ml of H_2SO_4 and 5 ml HNO_3). The two dispersions were mixed together and left for 10 min. The mixture was sonicated for 3 hours and then centrifuged for 1 hour at 22000 rpm. The supernatant was decanted and distilled water was added to the graphene pellets. In the next step, the solution was centrifuged again for 1 hour at 22000 rpm. This process was repeated five times until the solution reached a pH of 7. Finally, the supernatant was decanted and ethanol was added to the graphene pellets. Finally, the graphene dispersed in ethanol was centrifuged, decanted and allowed to dry. 0.75 mg of the obtained GO was dissolved in 1 ml distilled water

and used as a stock solution. GO dispersions were kept at room temperature and sonicated for 10 min prior to use.

2.4. Preparation of nCe labeled OTA (nCe-OTA)

To modify the OTA with nCe, 2 µl of 1.25 mg/ml OTA was diluted with 248 µl of distilled water, and varying volumes of diluted OTA were mixed with 100 µl of 10% cerium oxide (IV). The mixture was incubated for 2 days to attach the OTA on the nCe surface. After 2 days of incubation, the mixture was centrifuged to precipitate the particles. Subsequent washing steps were performed to eliminate the unbound OTA. Afterwards, the supernatant was removed. The resulting nCe-OTA conjugate was dispersed in 500 µl of distilled water.

2.5. Surface modification of SPCE electrodes and aptasensor fabrication

15 µl of 0.75 mg/ml GO dissolved in water was coated onto the SPCE surface. 15 µl of 10 mg/ml EDC dissolved in binding buffer was added onto the surface to activate terminal carboxylic groups of the carboxylated graphene for covalent coupling through the amino group of the 5'-amino-modified aptamer. Subsequently, 15 µl of 5'-amino-modified aptamer (18.8 µM) was immobilized onto the surface of the GO through an amidation reaction. After 1 hour incubation at room temperature, the modified SCPEs were washed with binding buffer to eliminate non-specific binding between the aptamer and the electrode surface. Finally, 10 µl of varying concentrations of free OTA (0.001 nM-180 nM) or the nCe-OTA (25 µl) were dropped onto the electrode surface and captured by the aptamer via the specific aptamer-target analyte interaction.

2.6. Real sample analysis

Non-contaminated corn samples (Potsdam, NY) were finely ground in a household blender to obtain corn powder. Aliquots (0.5 g) of the corn powder were spiked with OTA at different concentrations and vortexed as follows. 5 ml of extraction solvent (methanol: water, 6:4 (v/v)) was first added, and then the sample was mixed using an orbital shaker for 30 mins at room temperature. After centrifugation for 10 min, the extract was used for analysis. For statistical analyses, three separate samples with different concentrations of OTA were prepared and each

concentration level was analyzed in three replicates. The relative standard deviation was used to evaluate the precision of the assay.

3.Results and Discussion

3.1. Method principle

Scheme 1 depicts the sensing principle of the non-enzymatic nCe based aptasensor. To fabricate the sensor, the electrode was first coated with GO to increase the aptamer loading and to amplify the electrochemical signal. The aptamer was then immobilized on the surface of GO via amide bond formation between the 5'-amino-modified aptamer and the carboxylic acid groups of the GO using EDC chemistry. To perform analysis, the target analyte (OTA) was captured by the immobilized aptamer via a specific competitive mechanism between the free and nCe labeled target. The binding event was assessed by measuring the catalytic activity of the surface attached nCe label as a result of the specific biorecognition. We used H_2O_2 to assess the catalytic activity of nanoceria, and to monitor the electrochemical response of the aptasensor as a result of the target analyte binding. The catalytic activity of nCe against H_2O_2 has been previously demonstrated.[12, 18] Amplification of the electro-oxidation of H_2O_2 by nCe can be measured electrochemically.[12] The high conductivity of GO and its peroxidase-like activity is expected to enhance the catalytic conversion and act synergistically with nCe. GO also facilitates the electron transfer between the catalytic label and the electrode surface further increasing detection sensitivity. As a proof of concept, the proposed strategy was employed to construct an electrochemical aptasensor for the detection of OTA.

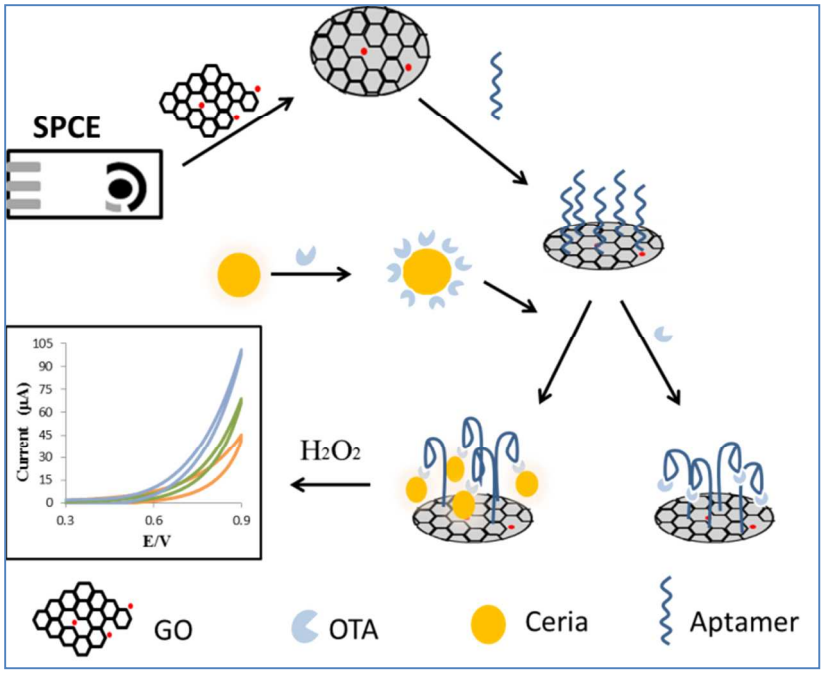

Scheme 1. Schematic illustration of the non-enzymatic nanocatalyst based electrochemical aptasensor concept involving the use of a nCe tag and GO.

3.2. Optimization of the nanoceria based aptasensor

3.2.1.Modification of nCe with OTA. The first step in the development of the sensor was to prepare the OTA conjugate probe on nCe. The TEM analysis shows spherical crystalline particles composed of 5 nm nanocrystals with an average size of ~ 20 nm (Figure 1A). The redox reactivity of nCe is directly related to the particle size. nCe particles of ~ 20 nm have previously shown enhanced surface reactivity against H_2O_2 and dopamine as compared to larger size particles of ~ 100 nm.[18, 19] Since the peak current is directly related to the surface reactivity of these particles, the commercially available 20 nm nCe were selected for this study. OTA was attached to the particle surface by electrostatic adsorption via its phenolic hydroxyl group and metal chelating properties. In previous work, we have demonstrated binding of phenolic compounds to nCe with formation of surface complexes though hydroxyl functionalities.[20] Here, we use this binding to attach OTA to nCe. To demonstrate the successful attachment of OTA to

nCe, OTA solutions were analyzed by UV-VIS spectroscopy in the absence and presence of nCe (Figure 1B). A distinct absorption peak characteristic of OTA was observed around 330 nm (curve a). In the presence of nCe a significant decrease in the absorption was seen with the same concentration of OTA (curve b) which can be attributed to the strong attachment of OTA to the particle surface. The labeling of OTA on the nanoceria surface was further confirmed by zeta potential analysis of the nanoparticle suspension upon addition of OTA. The bare ceria particles have a zeta potential value of +34.5(±3.4) mV. The particles exposed to OTA showed a decreased zeta potential of +26(±1.4) mV, indicating surface attachment of analyte on the nanoparticle surface (Table S1). Additionally, the average diameter of the particles as determined by dynamic light scattering (DLS) increased from 22(±1.1) to 25.4(±1.3) nm with the addition of OTA, suggesting binding of analyte (Table S1). The presence of OTA onto nCe was corroborated by thermogravimetric analysis (TGA) of the particles exposed to OTA after washing and drying (Figure 1C). The TGA of the OTA-nanoceria sample showed a gradual weight loss at a temperature higher that 180 C° which corresponds to the thermal decomposition of OTA. This demonstrates a strong binding between the OTA and nCe.

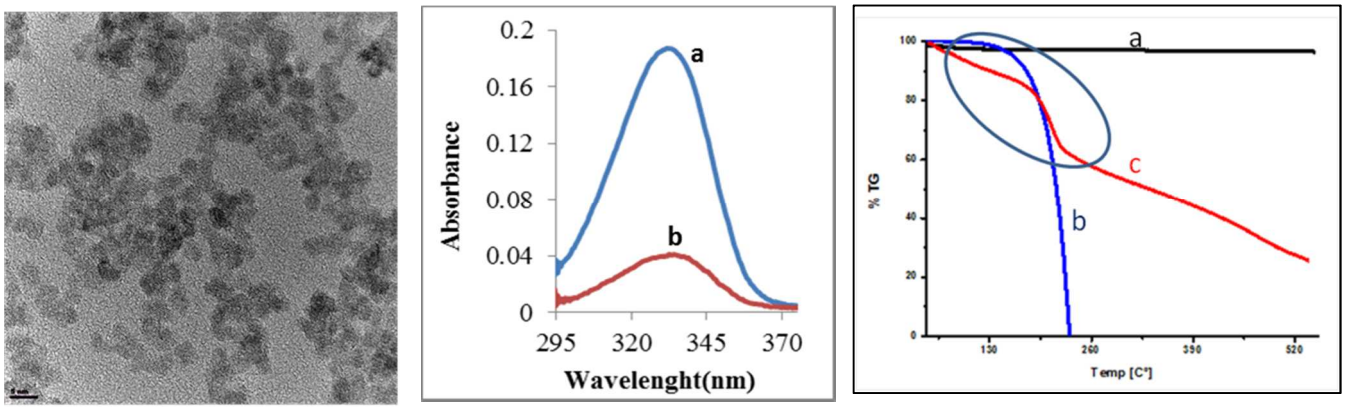

A B C

Figure 1. A: TEM image of nCe particles used in this work. B. Absorption spectra of 0.05 mM OTA in the a) absence and b) presence of nCe particles (16.5 mg/mL). C: Thermogravimetric analysis of: a) nCe particles, b) OTA, c) nCe-OTA complex.

3.2.2. Electrochemical characterization of the electrode surface. To characterize the electrode surface, we first performed cyclic voltammetry (CV) and electrochemical-impedance

spectroscopy (EIS) studies to determine changes in the electrochemical properties with each modification step. Figure 2 presents Nyquist diagrams of the EIS spectrum for different modification steps at the SPCE surface in the presence of 1 mM $K_3[Fe(CN)_6]$ used as a redox probe. The bare SPCE electrode revealed a low electron transfer resistance (R_{et}) value of 2.57 kΩ. For the electrode modified with GO, the R_{et} increased to 3.12 kΩ. This increase could be attributed to the negatively charged COO^- of the GO layers which can act as an electrostatic barrier and reduce the ability of the redox probe to access the conductive GO layer. [21-22-23] Activation of the terminal carboxylic group by EDC resulted in a decrease in R_{et} (0.01 kΩ) compared to the GO modified electrode. Replacement of the carboxyl group by the o-acylisourea intermediate at the GO surface promoted the electron transport of the redox probe to the electrode surface. Further covalent immobilization of the aptamer onto the GO-EDC electrode modified via amide bond formation resulted in an increased R_{et} (1.73 kΩ). Since both the backbone phosphate group of the aptamer and the $K_3[Fe(CN)_6]$ have negative charges, electrostatic repulsion between the phosphate group of the modified electrode and $K_3[Fe(CN)_6]$ dominate. $K_3[Fe(CN)_6]$ did not intercalate into the aptamer structure,[24] which may hinder the ability of the redox probe to access the electrode surface. Binding of OTA to the surface-bound aptamer increased the R_{et} to 3.5 kΩ. This increase could be related to an electrostatic blocking effect induced by the presence of the anionic carboxyl (COO^-) and phenolic functional ($Ph\text{-}O^-$) groups[25] in the OTA structure, hindering the electron transfer at the surface-bound OTA. Structural changes of oligunocleotide upon binding to the analyte can also affect the efficiency of the electron transfer kinetics and increase the R_{et}. It is expected that the aptamer changes conformation upon binding to the target OTA, also affecting the charge transfer kinetics to the electrode surface.[26] The electrochemical impedance spectra were fitted with a Randles equivalent circuit. This circuit consisted of ohmic resistance (R_s) of the electrolyte, the electron transfer resistance (R_{et}), Warburg impedance (Z_w) around each electrode and the constant phase element (Q_{dl}) (Figure 2, inset). The two elements of the equivalent electric circuit, R_s and Z_w, correspond to the properties of the bulk solution and the diffusion of the redox probe; they will not be affected by the reaction taking place at the electrode surface. The Q_{dl} represents the diaelectric constant of the layer, the surface area of the electrode and the thickness of the separation layer. For the insulating features at the electrochemical transducer interface, the prominent change was found in R_{et}, indicating that assembly of the aptamer-OTA

complex on the electrode surface introduces an electron transfer barrier. Thus, R_{et} was choosen as a suitable parameter for investigating the interfacial properties of the prepared aptasensor during all of the fabrication steps.

CV in the $K_3[Fe(CN)_6]$ solution was further used to monitor the electrochemical behavior of the modified electrode and complement the EIS studies. The voltammograms for each modification step are shown in Figure 2B. The CV of the bare SPCE showed the characteristic quasi-reversible anodic and cathodic peak potentials of $[Fe(CN)_6]^{4-/3-}$. The GO modified electrode did not show a significant change as compared to the bare SPCE. However, the current increased signifigantly after EDC treatment of the terminal carboxylic group of GO, in accordance with EIS results. Further immobilization of the aptamer on the GO-EDC electrode induced a decrease in the peak current potentially due to electrostatic repulsion between the backbone phosphate group of the aptamer and the $[Fe(CN)6]^{3-/4-}$redox probe. Binding of OTA to the immobilized aptamer further decreased the peak current and induced a shift of the redox potentials with a wider peak to peak separation compared to the GO-aptamer electrode. These changes were consistent with those observed by EIS and demonstrate successful modification of the electrode surface and OTA binding to the surface immobilized aptamer. SEM analysis show changes in the morphology of the electrode surface at each fabrication step (Figure S1).

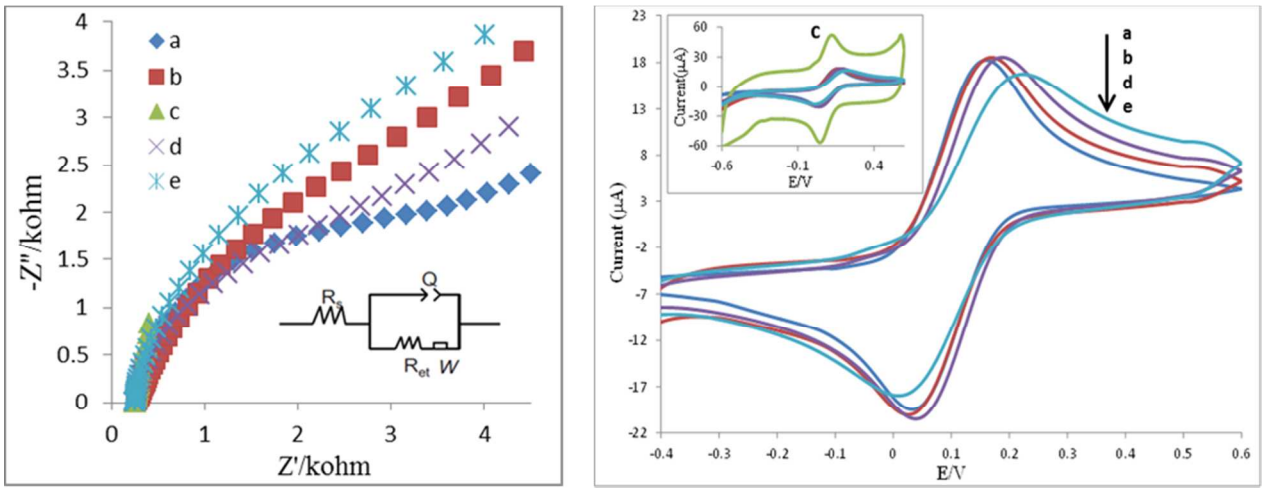

A **B**

Figure 2. Nyquist plots (A) and CV (B) of 1 mM $K_3[Fe(CN)_6]$ for: a) Bare b) Bare/GO c) Bare/GO/EDC d) Bare/GO/EDC/apt e) Bare/GO/EDC/apt/OTA.

3.3. Electrochemical detection: sensing principle and optimization of experimental parameters. In the proposed aptasensor design, nCe is used as a label to monitor the aptamer – OTA interaction at the GO modified electrode via a competitive detection mechanism. H_2O_2 was used to monitor the catalytic activity of the nCe-OTA captured on the aptamer-GO surface. We hypothesize that the sensitivity of the aptasensor could be greatly enhanced by using nCe as a catalytic label, and by measuring its catalytic activity against H_2O_2. Furthermore, GO has been reported to possess peroxidase like activity, further amplifying the H_2O_2 signal and enhancing detection sensitivity of the OTA-aptamer binding event. Figure 3 shows the H_2O_2 oxidation current for the bare, GO, GO/EDC, GO/EDC/Aptamer, GO/EDC/Aptamer/OTA and the GO/EDC/Aptamer/nCe labeled OTA electrodes in binding buffer. A significant increase in the H_2O_2 oxidation current was obtained for the GO coated electrode, compared to the bare electrode. This current further increased after activation with EDC. This can be attributed to the high conductivity and the electrocatalytic behavior of GO for H_2O_2.[27] Further covalent attachment of the aptamer decreased the oxidation current; the presence of the aptamer on the electrode surface hindered the flow of electrons to access the conductive layer. A further decrease was observed following OTA binding at the aptamer modified electrodes, which could be partly due to conformational changes of the immobilized aptamer after the binding of its target analyte. However, a significant increase in current was seen after the capture of the nCe-OTA probe by the aptamer. The increase in the electro-oxidation current of H_2O_2 demonstrates the catalytic amplifcation provided by the nCe particles.

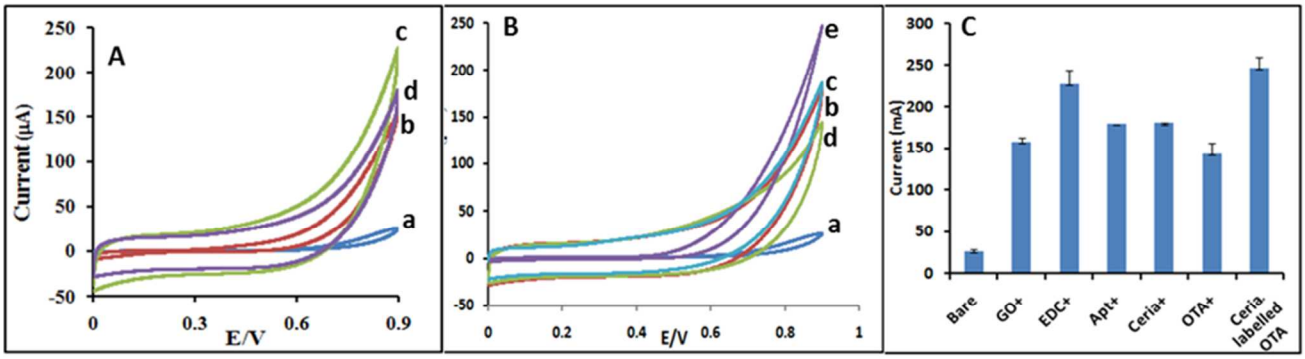

Figure 3. CVs of 0.2 M H_2O_2 at a scan rate of 0.1 V/s for **A)** a) Bare b) Bare/GO c) Bare/GO/EDC d) Bare/GO/EDC/apt **B)** a) Bare b)Bare/GO/EDC/apt c) Bare/GO/EDC/apt/free

nCe c) Bare/GO/EDC/apt/OTA d) Bare/GO/EDC/apt/nCe labeled OTA. **C)** Corresponding bar graphs.

To further evaluate the role of nCe, experiments were carried out to determine the optimum particle concentration in the presence of a constant amount of H_2O_2. CVs of different concentrations of nCe at the GO-apt modified electrode showed an increase in the anodic oxidation peak starting from around 0.45 V. This peak corresponds to the oxidation of H_2O_2. The amplitude of this current is proportional to the nanoceria concentration (Figure 4). The optimal concentration of nCe of 16.5 mg/mL was further employed to optimize the other experimental parameters. Subsequently, the experiments were performed to determine the OTA concentration for nCe modification. CVs of the H_2O_2 oxidation as a function of OTA concentration (Figure S2) showed an increase in the oxidation current with increasing OTA concentration. The higher current seen with the highest concentration of OTA on nCe is due to the increase binding of the nCe-OTA complex to the immobilized aptamer, and subsequently the presence of a higher amount of catalyst on the electrode surface. The maximum electrochemical response was achieved with 45 μM OTA, the sensor reached a saturation point at this value. Further experiments were conducted to optimize the concentration of nCe modified OTA. The effect of the nCe-OTA concentration was determined by monitoring the H_2O_2 oxidation current at 0.9 V The current responded linearly to additions of nCe-OTA (Figure S3), The reaction proceeds almost instantaneously and the electrochemical signal is stable; no change in the oxidation current was observed following 20 min of incubation of the nCe-OTA with H_2O_2 (Figure S4). Thus, the designed aptasensor can be used without further incubation.

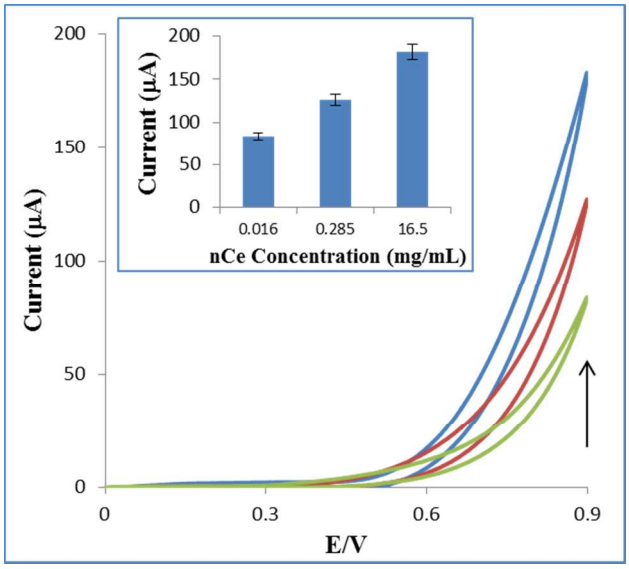

Figure 4. Concentration dependent increase of the H_2O_2 (0.2 M) oxidation with varying nCe concentrations (0.016, 0.28 and 16.5 mg/mL). The inset shows the current recorded at 0.09 V as a function of nCe concentration.

3.4. Aptasensor performance and study of interferences

Under the optimized conditions (16.5 mg/mL ceria labeled 45 µM OTA, 0.2 M H_2O_2), a quantitative measurement of OTA was performed by direct competition between the nCe-OTA and free OTA. The GO/Aptamer modified aptasensor was exposed to various concentrations of free OTA in the presence of a similar amount of nCe-OTA. The addition of free OTA decreased the current intensity due to inhibition of binding by the nCe labeled conjugate probe to the immobilized aptamer, leading to decrease of the H_2O_2 oxidation signal. Competitive calibration curves using standard solutions of OTA (from 0.001 nM to 180 nM) under the optimized conditions (Figure 5) revealed a concentration dependent response of the H_2O_2 oxidation current in the range of 0.15 to 50 nM. The corresponding CVs are presented in the Figure S5. Due to the relative standard deviation (5%) associated with the aptasensing platform, the detection threshold was considered at 85% binding. The detection limit was calculated to be 0.1 nM which is below the concentration limit of OTA in raw cereals grains (5 µg/kg), and products derived from cereals (3 µg/kg) according to the European Union regulations (EC No 123/2005). The obtained

LOD is also lower than that reported for previously used ELISA based affinity (e.g. immuno, aptamer) assays for OTA detection (Table S2).

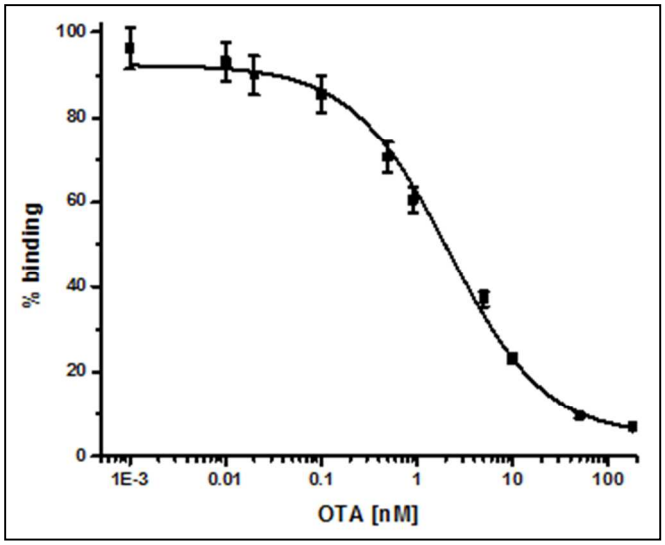

Figure 5. Competitive calibration curves using standard solutions of OTA (from 0.001 nM to 180 nM) under the optimized conditions.

The target selectivity is another important analytical performance parameter of the designed sensor. A control experiment was performed to evaluate the target specific detection of the electrochemical aptasensor. Instead of the original analyte, the response of the sensor to a close interfering analyte, Ochratoxin B (OTB), was tested. No electrochemical change in the H_2O_2 oxidation current was observed after addition of OTB to the OTA specific aptasensor platform for three different OTB concentrations (Figure 6). This shows that the presence of free OTB had no effect on the binding event of the nanoceria modified OTA conjugate probe for the immobilized aptamer, demonstrating specificity of the method against OTB. The reproducibility of the proposed assay was evaluated with interassay precision. The interassay precision was carried out using the same concentration of OTA for three aptasensors independently prepared under similar experimental conditions. A relative standard deviation of 2-4% (n=6) was observed, revealing acceptable precision and fabrication reproducibility.

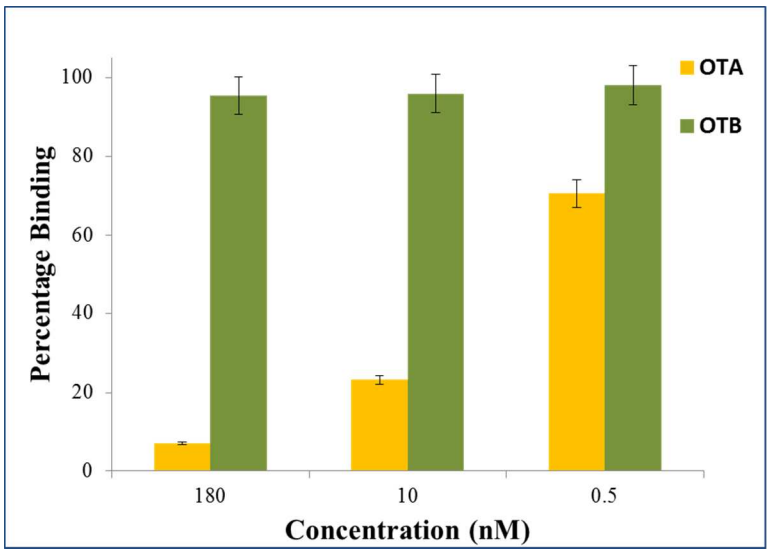

Figure 6. Comparison of percentage binding of ceria modified OTA in the presence of free OTA and OTB.

3.5. Application of the aptasensor to the detection of OTA in corn samples

To evaluate the analytical reliability of the proposed aptasensor for measurements of OTA, we have applied the method for the detection of OTA in corn samples. Assays were performed by spiking the corn sample with three different concentrations of OTA. The recovery was calculated on the basis of calibration curves performed in buffer. The percentage recoveries obtained were in good agreement with the spiked amounts of OTA (**Table 2**). The slight difference between the measured and real values could be due to the effect of the sample extract. Further studies to improve the extraction process are required. The recovery results for the developed aptasensor (Table 2) indicate that the proposed method can determine OTA presence in corn samples even at OTA concentrations lower than the limits allowed by the European Union. For example, in the European Union, regulatory limits for OTA in food products have been instated in products such as: raw cereal grains (5 µg/kg), dried fruits (10 µg/kg), roasted coffee and coffee products (5 µg/kg), and grape juice (2 µg/kg) (EC No. 123/2005).

3.6 Advantages of the nCe based affinity assay

Most commonly used affinity assays based on antibody or aptamer recognition rely on the use of enzymes as label to generate the signal. Enzymes have limited stability, require specific working conditions and are relatively expensive. Assays involving enzyme labels are complex, involve multistep procedures and complex enzymatic labeling, and many have decreased sensitivity. Efforts to overcome the sensitivity issue include the use of bienzymatic systems,[28] multi DNA strands,[29-31] polymerize chain reactions[32] and some involve several sequential experimental steps.[33] While these approaches have shown improved detection sensitivity, they have increased cost per assay and require multiple steps, making them difficult to implement for real time applications. Moreover, these methodologies still require sensitive labels and complex modification/labeling chemistries. Recently, with the advent of nanotechnology, nanomaterials such as gold and silver nanoparticles have been employed as signal generating probe to replace enzyme labels.[34] Signal generation of these assays is dependent on the aggregation and dispersion of the nanoparticles and may be affected by pH, ionic strength and temperature variations. Most of these assays have been designed for colorimetric and chemiluminscence detection which are in general less sensitive than electrochemical detection. As compared to previously described assays, the signal in the nCe based method described in this work relies on the redox surface chemistry of nCe particles, followed by the electrochemical quantification of the catalytic label. The detection was further amplified by the carboxyl GO layer used as electrode material to immobilize the aptamer and to increase the electron transfer rate at the electrode surface. The use of nCe as label brings significant advantages over other previously reported aptasensors including: 1) nCe is highly stable, inexpensive and a highly powerful catalyst, 2) it has rich surface functionalities in aqueous solutions that makes it amenable to modification, 3) can act as both a catalytic label and as a redox mediator. When combined with graphene oxide it provides a powerful amplification system. The high sensitivity, stability, and reproducibility of the assay combined with the low cost of nCe provide a unique design for the development of highly stable and sensitive aptasensors for field analysis. This approach is not only limited to OTA detection, as demonstrated in this work, but can easily be extended to other types of affinity assays.

4.Conclusion

In conclusion, we have developed a universal aptasensing platform using catalytically active nCe particles as a replacement for commonly used enzyme labels and electrochemical mediators in conventional affinity assays. To the best of our knowledge, this is the first use of redox active nCe particles as a catalytic label in electrochemical aptasensors. Furthermore, the synergistic effect between the catalase activity of nCe and the peroxidase like activity of GO increased the sensitivity of the assay for the detection of target analytes. The aptasensor displayed a very low detection limit for OTA, well below the regulatory limits. The high sensitivity, stability, and reproducibility of the assay combined with the low cost of nCE provide a unique design for the development of highly stable and sensitive aptasensors for field analysis. These characteristics add to the advantages of aptamers (e.g. high stability, ease of production and modification), making this design particularly appealing. This sensor format can be applied for the detection of other target analytes and can find broad applicability in the medical, environmental and food quality monitoring fields.

Acknowledgements

This material is based upon work supported by the National Science Foundation under Grant No. 0954919. Any opinions, findings, and conclusions or recommendations expressed in this material are those of the author(s) and do not necessarily reflect the views of the National Science Foundation.

References

1. H. Y. Kong and J. Byun, *Biomolecules & Therapeutics*, 2013, 21, 423-434.
2. A. D. Ellington and J. W. Szostak, *Nature*, 1990, 346, 818-822.
3. S. Song, L. Wang, J. Li, C. Fan and J. Zhao, *TrAC Trends in Analytical Chemistry*, 2008, 27, 108-117.
4. S. D. Jayasena, *Clinical Chemistry*, 1999, 45, 1628-1650.
5. Y. Zhang, J. P. Small, M. E. S. Amori and P. Kim, *Physical Review Letters*, 2005, 94, 176803.
6. K. S. Novoselov, A. K. Geim, S. V. Morozov, D. Jiang, M. I. Katsnelson, I. V. Grigorieva, S. V. Dubonos and A. A. Firsov, *Nature*, 2005, 438, 197-200.

7. Y. Zhang, Y.-W. Tan, H. L. Stormer and P. Kim, *Nature*, 2005, 438, 201-204.
8. Y. Song, K. Qu, C. Zhao, J. Ren and X. Qu, *Advanced Materials*, 2010, 22, 2206-2210.
9. T. Pirmohamed, J. M. Dowding, S. Singh, B. Wasserman, E. Heckert, A. S. Karakoti, J. E. S. King, S. Seal and W. T. Self, *Chemical Communications*, 2010, 46, 2736-2738.
10. C. Korsvik, S. Patil, S. Seal and W. T. Self, *Chemical Communications*, 2007, DOI: 10.1039/b615134e, 1056-1058.
11. D. Andreescu, G. Bulbul, R. E. Ozel, A. Hayat, N. Sardesai and S. Andreescu, *Environ-Sci Nano*, 2014, 1, 445-458.
12. C. Ispas, J. Njagi, M. Cates and S. Andreescu, *J. Electrochem. Soc.*, 2008, 155, F169-F176.
13. J. Njagi, C. Ispas and S. Andreescu, *Analytical Chemistry*, 2008, 80, 7266-7274.
14. A. Hayat and S. Andreescu, *Analytical Chemistry*, 2013, 85, 10028-10032.
15. M. L. Fernández-Cruz, M. L. Mansilla and J. L. Tadeo, *Journal of Advanced Research*, 2010, 1, 113-122.
16. A. Pfohl-Leszkowicz and R. A. Manderville, *Molecular Nutrition & Food Research*, 2007, 51, 61-99.
17. V. A. Chhabra, A. Deep, R. Kaur and R. Kumar.
18. M. Ornatska, E. Sharpe, D. Andreescu and S. Andreescu, *Analytical Chemistry*, 2011, 83, 4273-4280.
19. A. Hayat, J. Cunningham, G. Bulbul and S. Andreescu, *Ana. Chim. Acta*, 2015, in press.
20. E. Sharpe, T. Frasco, D. Andreescu and S. Andreescu, *Analyst*, 2013, 138, 249-262.
21. A. Hayat, L. Barthelmebs and J.-L. Marty, *Sensors and Actuators B: Chemical*, 2012, 171–172, 810-815.
22. G. Yang, W. Jin, L. Wu, Q. Wang, H. Shao, A. Qin, B. Yu, D. Li and B. Cai, *Analytica Chimica Acta*, 2011, 706, 120-127.
23. P. Geng, X. Zhang, W. Meng, Q. Wang, W. Zhang, L. Jin, Z. Feng and Z. Wu, *Electrochimica Acta*, 2008, 53, 4663-4668.
24. G. S. Bang, S. Cho and B.-G. Kim, *Biosensors and Bioelectronics*, 2005, 21, 863-870.
25. A.-E. Radi, X. Muñoz-Berbel, V. Lates and J.-L. Marty, *Biosensors and Bioelectronics*, 2009, 24, 1888-1892.
26. S. Pilehvar, T. Dierckx, R. Blust, T. Breugelmans and K. De Wael, *Sensors (Basel, Switzerland)*, 2014, 14, 12059-12069.
27. S. Palanisamy, S. M. Chen and R. Sarawathi, *Sensor Actuat B-Chem*, 2012, 166, 372-377.
28. L. Bai, R. Yuan, Y. Chai, Y. Yuan, Y. Zhuo and L. Mao, *Biosensors and Bioelectronics*, 2011, 26, 4331-4336.
29. L. Huang, J. Wu, L. Zheng, H. Qian, F. Xue, Y. Wu, D. Pan, S. B. Adeloju and W. Chen, *Analytical Chemistry*, 2013, 85, 10842-10849.
30. Y. Yuan, S. Wei, G. Liu, S. Xie, Y. Chai and R. Yuan, *Analytica Chimica Acta*, 2014, 811, 70-75.
31. L. Jiang, J. Qian, X. Yang, Y. Yan, Q. Liu, K. Wang and K. Wang, *Analytica Chimica Acta*, 2014, 806, 128-135.
32. X. Zhu, J. Zhao, Y. Wu, Z. Shen and G. Li, *Analytical Chemistry*, 2011, 83, 4085-4089.
33. Z. Chen, L. Li, Y. Tian, X. Mu and L. Guo, *Biosensors and Bioelectronics*, 2012, 38, 37-42.
34. I. Palchetti and M. Mascini, *Anal Bioanal Chem*, 2012, 402, 3103-3114.

Figure Captions

Scheme 1. Schematic illustration of the non-enzymatic nanocatalyst based electrochemical aptasensor concept involving the use of a nCe tag and GO.

Figure 1. Absorption spectra of 0.05 mM OTA in the a) absence and b) presence of nCe particles (16.5 mg/mL).

Figure 2. Nyquist plots (A) and CV (B) of 1 mM $K_3[Fe(CN)_6]$ for: a) Bare b) Bare/GO c) Bare/GO/EDC d) Bare/GO/EDC/apt e) Bare/GO/EDC/apt/OTA.

Figure 3. CVs of 0.2 M H_2O_2 at a scan rate of 0.1 V/s for **A)** a) Bare b) Bare/GO c) Bare/GO/EDC d) Bare/GO/EDC/apt **B)** a) Bare b)Bare/GO/EDC/apt c) Bare/GO/EDC/apt/free nCe c) Bare/GO/EDC/apt/OTA d) Bare/GO/EDC/apt/nCe labeled OTA. **C)** Corresponding bar graphs.

Figure 4. Concentration dependent increase of the H_2O_2 (0.2 M) oxidation with varying nCe concentrations (0.016, 0.28 and 16.5 mg/mL). The inset shows the current recorded at 0.09 V as a function of nCe concentration.

Figure 5. Competitive calibration curves using standard solutions of OTA (from 0.001 nM to 180 nM) under the optimized conditions.

Figure 6. Comparison of percentage binding of ceria modified OTA in the presence of free OTA and OTB.

Tables

Table 1. Oligonucleotide used in this work

5'-amino-modified aptamer	Sequence(5'→ 3') NH_2-GAT-CGG-GTG-TGG-GTG-GCG-TAA-AGG-GAG-CAT-CGG-ACA

Table 2. Application of the aptasensor in corn samples.

Sample No	Spiked OTA (nM)	Found OTA (nM)	RSD (%)	Recovery (%)
1	0.8	0.74	3.1	92.5
2	1.5	1.42	3.4	94.6
3	5	4.8	4.3	96